Title
Superconductivity in the Th0.93Zr0.07B12 compound with UB12 prototype structure

Journal
Physics Letters, Section A: General, Atomic and Solid State Physics, 379(39)

ISSN
0375-9601

Authors
Renosto, ST
Corrêa, LE
Da Luz, MS
et al.

Publication Date
2015-10-16

DOI
10.1016/j.physleta.2015.07.018

Physics Letters A 379 (2015) 2498–2501

Contents lists available at ScienceDirect

Physics Letters A

www.elsevier.com/locate/pla

Superconductivity in the $Th_{0.93}Zr_{0.07}B_{12}$ compound with UB_{12} prototype structure

S.T. Renosto [a], L.E. Corrêa [a], M.S. da Luz [a,b,*], P.F.S. Rosa [c], Z. Fisk [c], J. Albino-Aguiar [d], A.J.S. Machado [a]

[a] Departamento de Engenharia de Materiais, Escola de Engenharia de Lorena, Universidade de São Paulo-Lorena, SP 12602-810, Brazil
[b] Instituto de Ciências Exatas e Tecnológicas, Departamento de Engenharia Ambiental, Universidade Federal do Triângulo Mineiro, Uberaba, MG 38066-200, Brazil
[c] Department of Physics and Astronomy, University of California-Irvine, Irvine, CA 92697, USA
[d] Departamento de Física, Universidade Federal de Pernambuco, Recife, PE 38066-200, Brazil

ARTICLE INFO

Article history:
Received 17 April 2015
Received in revised form 11 July 2015
Accepted 13 July 2015
Available online 15 July 2015
Communicated by L. Ghivelder

Keywords:
Superconductivity
ThB_{12} system
New superconductors

ABSTRACT

In this work, we report superconductivity at 5.5 K in the new pseudo-ternary $Th_{0.93}Zr_{0.07}B_{12}$ compound. We show clearly evidence that appropriate amounts of Zr substitution at the Th site induce the stabilization of the UB_{12} prototype structure at ambient pressure. The superconducting bulk properties of $Th_{0.93}Zr_{0.07}B_{12}$ are confirmed by means of magnetization, electronic transport properties and specific heat measurements. The H–T phase diagrams based on magnetization and magnetoresistance measurements yield $\mu_0 H_{c1}(0) = 6$ mT and $\mu_0 H_{c2}(0) = 98$ mT and allow us to estimate the coherence length $\xi_0 \sim 57.9$ nm and the penetration depth $\lambda_L \sim 234$ nm at zero kelvin.

1. Introduction

The M–boron (M = lanthanides, actinides, and transition metals) binary systems host a few stoichiometric phases which crystallize in the UB_{12} prototype structure. At ambient pressure growth conditions, it is well known that this structure can be obtained with seven lanthanide elements ((Tb–Lu)B_{12}) [1–4], three actinide members (UB_{12}, NpB_{12}, and PuB_{12}) [5–7], and three transition metals (YB_{12}, ZrB_{12}, and ScB_{12}) [1,8–10]. These compounds have attracted a lot of scientific efforts due to their extraordinary range of electronic, magnetic and structural properties. For instance, HoB_{12}, ErB_{12}, and TmB_{12} compounds exhibit antiferromagnetic ordering, with Néel temperatures of 7.38, 6.65, and 3.28 K, respectively [11–14]; UB_{12} shows Pauli paramagnetism [15]; and YB_{12}, ZrB_{12}, ScB_{12}, and LuB_{12} have been addressed as superconducting materials [16–20].

In spite of this, several phases, such as ThB_{12}, with UB_{12} structure have been also obtained by using external hydrostatic pressure [21]. Since this work is the only one reporting the ThB_{12} phase existence, a lot of questions about its electronic and magnetic properties remain unclear.

Based on the mentioned above, in this work we report the influence of Zr doping in the ThB_{12} system. We show clear evidence that 7% of Zr substitution is already able to stabilize the ThB_{12} structure, under normal pressure conditions. Superconductivity was found to appear in this system with a maximum T_c (∼5.5 K) close to the $Th_{0.93}Zr_{0.07}B_{12}$ composition. From the penetration depth and coherence length values, the Ginzburg–Landau (GL) parameter (κ) was found to be 4.04. In addition, heat capacity measurements indicated a conventional superconductivity in this compound.

2. Experimental procedure

The samples were prepared from stoichiometric amounts of Th, Zr and B pieces (high purity >99.999%) which were melted on a water cooled Cu hearth in an arc furnace with high electrical current and elevated heat extraction, under high purity argon atmosphere and using a Ti sponge getter. The samples were flipped over and remelted 5 times to ensure good homogeneity. Due to the low vapor pressure of the constituent elements at the melting temperature, the weight loss during the arc melting was negligible (<0.5%). X-ray powder diffractograms were obtained in a Panalitycal diffractometer model Empyrean with detector PIXcel^{3D} using CuK_α radiation. The lattice parameters were determined by using the PowderCell software and simulation as well [22]. Magnetic data were obtained using a high sensitivity VSM-SQUID magnetometer from Quantum Design. The temperature dependence was obtained using a zero field cooling (ZFC) and field cooling (FC) sweeps with an applied DC magnetic field of 10 Oe. The M ver-

* Corresponding author.
E-mail address: daluz.mario@icte.uftm.edu.br (M.S. da Luz).

http://dx.doi.org/10.1016/j.physleta.2015.07.018

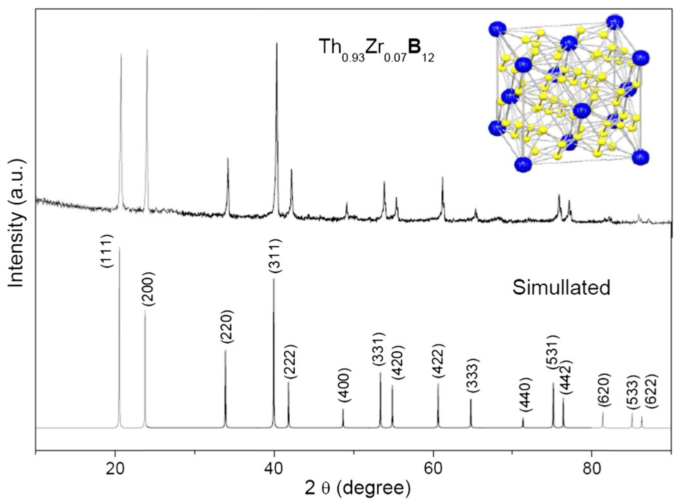

Fig. 1. (Color online.) Experimental (upper) and simulated (lower) X ray diffractions. In the inset we show the ThB_{12} crystal structure in which the blue spheres are Th and the yellow ones are B.

sus H measurement was performed at 2.0 K. Electrical resistivity measurements were made between 2.0 and 300 K with a conventional four probe method using an AC current bridge of 1000 μA in the PPMS-9T equipment. The resistivity data were obtained at zero field and at several applied magnetic fields in order to estimate the upper critical field. The specific heat of a piece cut from the sample was measured in the range of 1.8–10 K with a calorimeter in the PPMS (Quantum Design) using the relaxation method.

3. Results

The upper panel of Fig. 1 shows the X-ray powder diffraction pattern for the sample with $Th_{0.93}Zr_{0.07}B_{12}$ composition. Majority of the peaks can be indexed using the UB_{12} prototype structure, which belongs to the cubic *Fm-3m* space group with lattice parameter $a = 7.465$ Å [12]. To confirm this assumption, Fig. 1 also shows the simulated X-ray for the ThB_{12} structure (see lower panel). An excellent agreement is found between the experimental result and the simulated structure. Based on this, one can infer that the substitution of 7% of Th by Zr is able to stabilize the UB_{12} structure in the Th–B system, at ambient pressure conditions. In the inset we show the ThB_{12} crystal structure in which the blue spheres are Th and the yellow ones are B. The broadening is due to the size of the grain in our sample. Actually the grain size is relatively small because these samples come from melting process (as cast sample).

Surprisingly, this stable structure shows superconducting behavior, as can be seen in Fig. 2(a), which shows the magnetization as a function of temperature in the zero-field cooled (ZFC) and field cooled (FC) regimes sweeps with an applied field of 10 Oe. This figure displays a clear diamagnetic transition at 5.5 K. The hysteresis between ZFC and FC regimes indicates that $Th_{0.93}Zr_{0.07}B_{12}$ has weak flux pinning centers. Without correcting for the demagnetization or sample size effects, we estimate the superconducting volume fraction (ZFC) in this sample to be around 80.0% of perfect diamagnetism, indicative of possible bulk superconductivity.

Fig. 2(b) shows the resistivity as a function of temperature at zero magnetic field for a $Th_{0.93}Zr_{0.07}B_{12}$ polycrystalline sample. The sharp transition reflects the good quality of our polycrystalline sample. The onset of the superconducting transition at ∼5.5 K can be better seen in the inset of Fig. 2(b) which shows very good agreement with the magnetization measurement shown in Fig. 2(a).

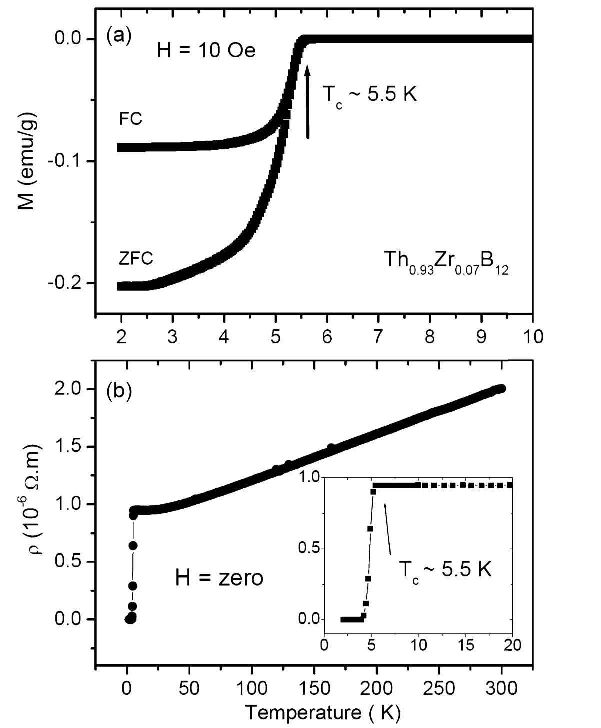

Fig. 2. (a) Magnetization as a function of temperature in the ZFC and FC regimes. A clear superconducting transition is observed close to 5.5 K. (b) Resistivity as a function of temperature at zero magnetic field. In the inset, one can see clearly the sharp superconducting transition at 5.5 K.

In order to estimate the lower critical field, the field dependence of the magnetization (*M* vs. *H*) was measured from 1.8 to 6.0 K as shown in Fig. 3(a). The values of H_{C1} were determined by examining the point of deviation from the linear slope of the magnetization curve, using $\Delta M = 10^{-3}$ eμ as a criterion for the difference between the Meissner line and magnetization signal (see Fig. 3(b)) [23].

From the data of Fig. 3(b), we are able to construct the $\mu_0 H_{c1}$ versus temperature diagram displayed in Fig. 4. The lower critical field as a function of the reduced temperature can be described in terms of a monotonic curve with a quadratic dependence dictated by the empirical function: $H_{c1}(T) = H_{c1(0)}(1 - t^2)$, where $t = T/T_c$. The fit of our data to this expression (solid red line) suggests that the vortex penetration in this material can be well described by BCS theory. By extrapolating the fit to zero Kelvin, we find that $\mu_0 H_{c1}$ is approximately 6 mT at zero temperature. Using this value ($\mu_0 H_{c1} \sim 6$ mT), it is possible to estimate the penetration depth using the formula $H_{c1} = \frac{\phi_0}{2\pi \lambda_L^2}$, where the λ_L parameter is the penetration depth $\lambda_L \sim 234$ nm, at zero Kelvin.

In order to estimate the upper critical field, Fig. 5(a) shows the normalized resistance as a function of magnetic field for a $Th_{0.93}Zr_{0.07}B_{12}$ polycrystalline sample. The resistance was normalized by the resistance value in the normal state to better determine the upper critical field (H_{c2}). As it can be seen in Fig. 5(a) the onset of superconductivity shifts to lower temperatures gradually with increasing magnetic field. The magnetoresistance behavior suggests a relatively small upper critical field (H_{c2}), consistent with the *M* vs. *T* and *M* vs. *H* curves. Using a criterion of 50% of normal state resistance, the estimated H_{c2}–T phase diagram shown in Fig. 5(b) was constructed. From the results shown in Fig. 5(b) we can estimate the upper critical field at zero temperature ($\mu_0 H_{c2(0)}$) using the WHH formula [24] in the limit of short electronic mean-free path (dirty limit), $\mu_0 H_{c2}(0) = -0.693(dH_{c2}/dT)_{T=T_c} T_c$. The zero temperature H_{c2} value of ∼98 mT was determined by extrapolating the red line to 0 K.

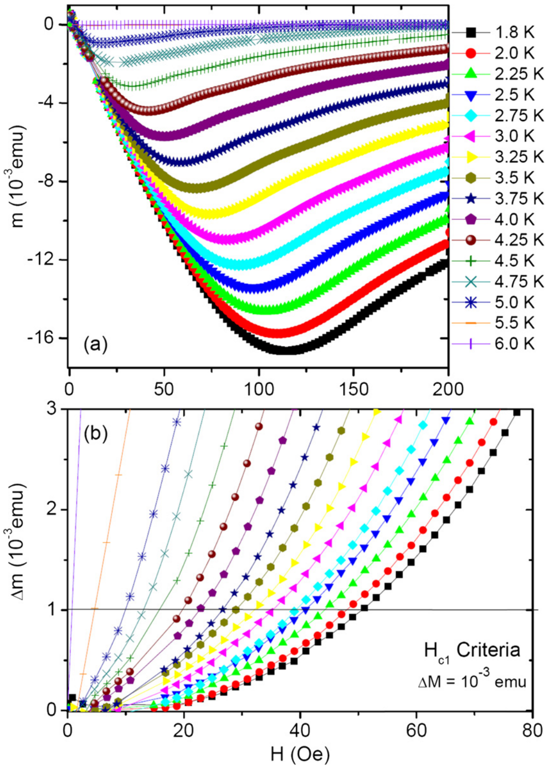

Fig. 3. (a) Magnetization as a function of applied magnetic field at several temperatures in the 1.8–6.0 K range. (b) ΔM vs. H used as criterion for the lower critical filed definition.

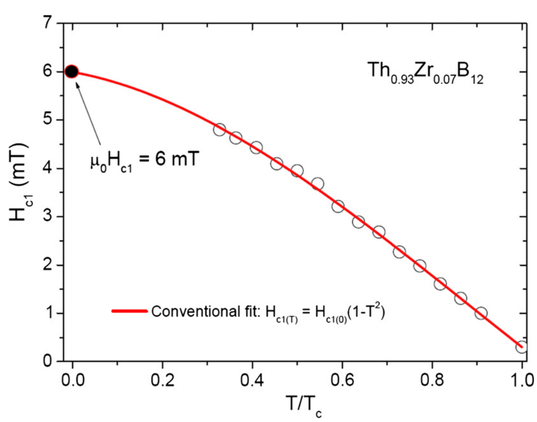

Fig. 4. (Color online.) $\mu_0 H_{c1}$ versus temperature showing the perfect fitting (red line) which suggests a lower critical field close to 6 mT at zero temperature.

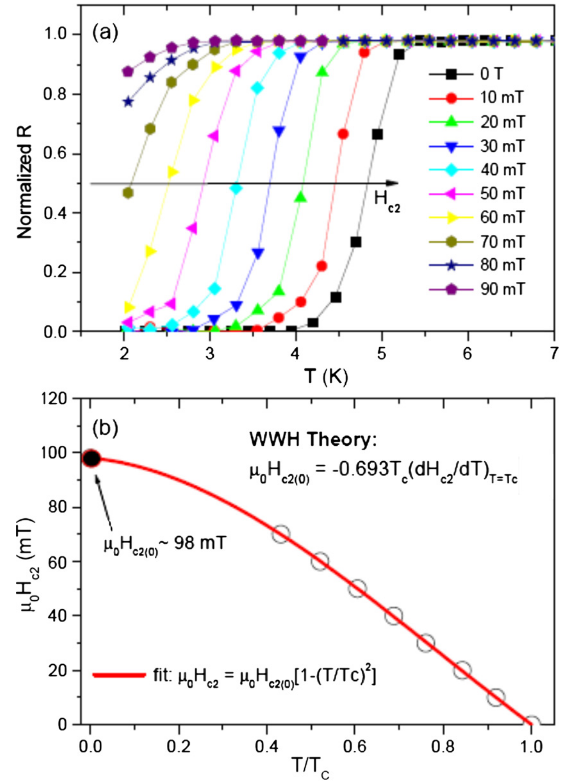

Fig. 5. (a) Normalized resistance as a function of applied magnetic field. (b) Upper critical field ($\mu_0 H_{c2}$) estimate from WHH theory (see text).

The upper critical field estimative from WHH (Fig. 5b) allows an estimation of the coherence length by using the Ginzburg–Landau (GL) formula: $\mu_0 H_{c2}(0) = \frac{\phi_0}{2\pi\xi_0^2}$, which yields $\xi_0 \sim 57.9$ nm. The penetration depth and coherence length give the GL parameter (κ) through the expression $\kappa = \frac{\lambda_0}{\xi_0} = 4.04$. Although this value ($\kappa = 4.04$) is much bigger than critical value ($\kappa_c = (1/2)^{1/2}$), conventionally used to classify superconductors as type-I or type-II, it is still low compared to the κ value typically obtained for type-II superconductors. For example, the $Zr_{0.96}V_{0.04}B_2$ compound is a type-II superconductor and shows $\kappa \sim 100$ [25].

Recently, theoretical studies have shown the existence of a very special superconductor type, which can have κ value in the vicinity of the theoretical limit value called "Bogomolny regime" [26], i.e., κ_c. In this regime, it is admitted that in the superconductor topological excitations are stable and vortices can attract one another at long range but repel at shorter ranges, and, therefore, should form clusters in low magnetic fields [27,28], these superconductors are currently classified as type-1.5 [28] or type-II/I [29,30]. More recently, Vagov et al. [31] showed that below T_c, in the $\kappa \times T_c$ phase diagram, there exists a critical range of T and κ parameters where the degeneracy of the superconducting state at T_c, that is at Bogomolny critical point, is lifted into a sequence of novel topological equilibria and based on this they defined a new class of superconducting materials, "the critical superconductors", that generalizes the types II/I and type-1.5. Based on this reasoning and the low-κ value obtained, we can suggest that the $Th_{0.93}Zr_{0.07}B_{12}$ compound can be one more example of this non-conventional type-II/I superconductor. Corroborating to this, the related ZrB_{12} compound has been also addressed as a type-II/I superconductor [29]. This material has $\kappa = 0.65$ and crosses over from type-I to type-II superconductivity close to 4 K with decreasing temperature. This assumption is very exciting, but specific heat and vortex imaging studies on single crystals should be done in order to confirm the type-II/I character of the $Th_{0.93}Zr_{0.07}B_{12}$ compound. It will also be interesting to have band structure calculation in order to guide the search of new compounds with the suggested behavior.

The bulk phase transition from the normal to the superconducting state in the $Th_{0.93}Zr_{0.07}B_{12}$ sample was also verified by specific heat measurements at low temperatures. A clear superconducting transition is observed in the C_p/T versus T^2 curve, presented in Fig. 6, where the critical temperature is observed close to 5.5 K, consistent with the resistivity and magnetization measurements. The normal state data can be fit to the expression $C_n = \gamma + \beta T^3$ by using a least-square analysis which yields $\gamma = 17.1$ (mJ/mol K^2) and $\beta = 0.22$ (mJ/mol K^4). This β value yields the Debye temperature $\Theta_D \sim 486$ K. The value of the Sommerfeld coefficient suggests high density of states at the Fermi level. By subtracting the phonon contribution, we are able to evaluate separately the electronic contribution to the specific-heat, plotted as C_e/T vs. T in the inset of

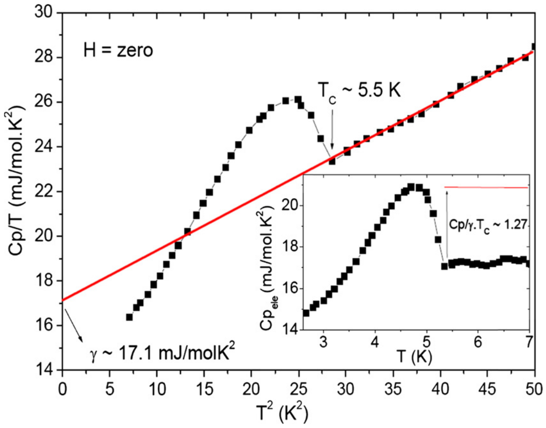

Fig. 6. Cp/T vs. T^2 displays a jump close to 30.2 K^2. The inset shows the electronic contribution for specific heat which reveal that the $\Delta C/\gamma T_c$ value is close to the BCS prediction (1.43).

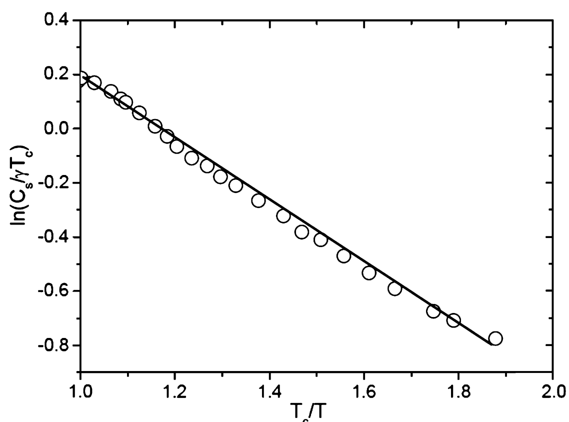

Fig. 7. C_s of $Th_{0.93}Zr_{0.07}B_{12}$ polycrystalline sample in the superconducting state is plotted in logarithmic scale vs. T/T_c, showing a behavior which agrees with BCS behavior.

Fig. 6. The analysis of the jump yields $\Delta C_e/\gamma_n T_c \sim 1.27$ which is somewhat close to BCS prediction of 1.43.

An analysis of the jump yields $\Delta C_e/\gamma_n T_c \sim 1.27$ which is somewhat close to BCS prediction (1.43), suggesting some conventional superconducting behavior in this material On the other hand, the related compound ZrB_{12} has been reported as a multiband superconductor [29].

The electronic heat capacity can be related to the nature of the superconducting state, especially, its temperature dependence is related to superconducting gap energy according to BCS theory ($C_e/\gamma_n T_c = ae^{-bT_c/T}$), where a and b are constants and b in the exponential heat capacity expression is one-half the band gap energy 1.25). Fig. 7 shows the C_e/γ_n versus T_c/T for the measurement presented in Fig. 6. If the slope of the experimental curve is determined by scaling, we can estimate an energy gap of 0.8 meV. This value is in according to conventional superconductor materials.

Finally, despite the discussions about the origin of superconductivity, or on the low value of Ginzburg–Landau κ_0 parameter, the results shown in this report indicate that the substitution of Th by Zr stabilizes the ThB_{12} compound at ambient pressure with a structure represented by the UB_{12} prototype and a bulk superconducting state with critical temperature of 5.5 K.

4. Conclusion

In this paper, we show that 7% of Zr is able to stabilize the ThB_{12} phase, with UB_{12} type structure at ambient pressure. We also report that this phase becomes superconducting below 5.5 K with the parameters $\mu_0 H_{c1}(0) = 6$ mT, $\mu_0 H_{c2}(0) = 98$ mT, $\xi_0 \sim$ 57.9 nm and $\lambda_L \sim 234$ nm, at zero Kelvin. The heat capacity data agree with BCS theory which could indicate conventional superconducting behavior in this material.

Acknowledgements

This material is based upon work supported by the FAPESP (2011/05961-3, 2014/01581-0, 2013/20181-0), NAP-USP, FAPEMIG, CNPq (448041/2014-6, 300821/2012-3) and CAPES (CAPES/CNPq PVE A10/2013), to which the authors wish to express their thanks. We would like also thank A. Shanenko and A. Vagov for stimulating discussions.

References

[1] S. LaPlaca, I. Binder, B. Post, J. Znorg. Nucl. Chem. 18 (1961) 113–117.
[2] S. LaPlaca, D. Noonan, Acta Crystallogr. 16 (1963) 1182.
[3] K. Schwetz, P. Ettmayer, R. Kieffer, A. Lipp, Radex Rundschaw (1972) 257–265.
[4] J.F. Cannon, D.M. Cannon, H.T. Hall, J. Less-Common Met. 56 (1977) 83–90.
[5] F. Bertaut, P. Blum, C. R. Acad. Sci. 229 (1949) 666–667.
[6] H.A. Eick, Inorg. Chem. 4 (1965) 1237–1239.
[7] H.A. Eick, R.N.R. Mulford, J. Inorg. Nucl. Chem. 31 (1969) 371–375.
[8] B. Post, F.W. Glaser, J. Met. 4 (1952) 631–632.
[9] V.I. Matkovich, J. Economy, R.F. Giese, R. Barrett, Acta Crystallogr. 19 (1965) 1056–1058.
[10] V.A. Bruskov, L.V. Zavalii, Y.B. Kuz'ma, Inorg. Mater. 24 (1988) 420–421.
[11] A. Czopnik, N. Shitsevalova, A. Krivchikov, V. Pluzhnikov, Y. Paderno, Y. Onuki, J. Solid State Chem. 177 (2004) 507–514.
[12] A. Kohout, I. Batko, A. Czopnik, K. Flachbart, S. Matas, M. Meissner, Y. Paderno, N. Shitsevalova, K. Siemensmeyer, Phys. Rev. B 70 (2004) 224416.
[13] A.V. Bogach, S.V. Demishev, K. Flachbart, S. Gabani, V.V. Glushkov, A.V. Levchenko, N. Shitsevalova, D.N. Sluchanko, N.E. Sluchanko, Solid State Phenom Ser. 152–153 (2009) 45–48.
[14] A.V. Bogach, S.V. Demishev, V.V. Glushkov, A.V. Levchenko, N. Shitsevalova, K. Flachbart, N.E. Sluchanko, J. Phys. Conf. Ser. 150 (2009) 041011.
[15] M. Kasaya, F. Iga, K. Katoh, K. Takegahara, T. Kasuya, J. Magn. Magn. Mater. 90 (1990) 521–522.
[16] Z. Fisk, A.C. Lawson, B.T. Matthias, E. Corenzwit, Phys. Lett. A 37 (1971) 251–252.
[17] B.T. Matthias, T.H. Geballe, K. Andres, E. Corenzwit, G.W. Hull, J.P. Mata, Science 159 (1968) 530.
[18] K. Hamada, M. Wakata, N. Sugii, K. Matsuura, K. Kubo, H. Yamauchi, Phys. Rev. B 48 (1993) 6892–6898.
[19] A. Czopnik, N. Shitsevalova, V. Pluzhnikov, A. Krivchikov, Y. Paderno, Y. Onuki, J. Phys. Condens. Matter 17 (2005) 5971–5985.
[20] K. Siemensmeyer, K. Flachbart, S. Gabani, S. Matas S, Y. Paderno, N. Shitsevalova, J. Solid State Chem. 179 (2006) 2748–2750.
[21] J.F. Cannon, P.B. Farnsworth, J. Less-Common Met. 92 (1983) 359–368.
[22] W. Kraus, G. Nolze, J. Appl. Crystallogr. 29 (1996) 301–303.
[23] S.L. Li, H.H. Wen, Z.W. Zhao, Y.M. Ni, Z.A. Ren, G.C. Che, H.P. Yang, Z.Y. Liu, Z.X. Zhao, Phys. Rev. B 64 (2001) 094522.
[24] N.R. Werthamer, E. Helfand, P.C. Hohenberg, Phys. Rev. 147 (1966) 295–302.
[25] S.T. Renosto, H. Consoline, C.A.M. dos Santos, J. Albino Aguiar, Soon-Gil Jung, J. Vanacken, V.V. Moshchalkov, Z. Fisk, A.J.S. Machado, Phys. Rev. B 87 (2013) 174502.
[26] E.B. Bogomolny, Sov. J. Nucl. Phys. 24 (1976) 449.
[27] J. Carlström, E. Babaev, M. Speight, Phys. Rev. B 83 (2011) 174509.
[28] V.V. Moshchalkov, M. Menghini, T. Nishio, Q.H. Chen, A.V. Silhanek, V.H. Dao, L.F. Chibotaru, N.D. Zhigadlo, J. Karpinski, Phys. Rev. Lett. 102 (2009) 117001.
[29] Yuxing Wang, Rolf Lortz, Yuriy Paderno, Vladimir Filippov, Satoko Abe, Ulrich Tutsch, Alain Junod, Phys. Rev. B 72 (2005) 024548.
[30] V.A. Gasparov, N.S. Sidorov, I.I. Zver'kova, Phys. Rev. B 73 (2006) 094510.
[31] A. Vagov, A.A. Shanenko, M.V. Milosevic, V.M. Axt, V.M. Vinokur, F.M. Peeters, arXiv:1311.5624.